Optimization of Cooperative *In Vivo* Sensor Network Operating at Terahertz Frequency

Monica Kaushik, *Graduate Student Member, IEEE*, Sindhu Hak Gupta, and Vipin Balyan

***Abstract*—In the current work, performance of cooperative as well as non-cooperative In Vivo sensor networks operating at terahertz frequency has been analyzed in terms of received power and energy. The human body as a wireless medium impacts signal propagation. Human tissues such as blood, fat, skin and water offer different permittivity to the signal. In this work a mathematical model has been formulated for cooperative and non-cooperative In Vivo sensor network where the dependence of received power and SNR on various parameters has been evaluated. A data set comprising of permittivity, pathloss and distance has been created from the proposed model. To optimize received power and energy, ANN is implemented, and the minimum error value of SNR is obtained which is further used to find optimized received power and energy for the In Vivo network under the considered scenario. Simulation results reveal that received power in the cooperative In Vivo network is increased by approx. 22% in the skin, 18%, in blood, 27% in water and 11% in fat and received energy is also increased by approx. 75% in comparison with the non-cooperative In Vivo network. It also has been noted that in comparison to other human tissues skin is the best medium for cooperative as well as non-cooperative scenario. Further optimized received power is increased by 37 % and 49 % for the non-cooperative and cooperative scenario respectively. Optimized received energy is increased by 11% and 20% for non- cooperative and cooperative scenario respectively.**

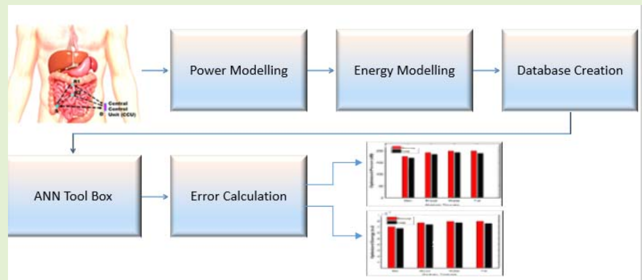

***Index Terms*—ANN, cooperative communication, human tissues, *in vivo*, optimization, WBAN.**

I. Introduction

RECENT advances in wireless communication make Wireless Body Area Networks (WBAN) a dynamic field of research in the healthcare sector [1]. WBANs are capable of providing continuous monitoring of various physiological parameters of patients proving beneficial for the aged and lonely subjects [2]. WBAN is comprised of sensor nodes that generally communicate wirelessly with one another [3]. As per the requirement of the parameters to be monitored sensor nodes may be deployed on the body, off the body, or in the body of a subject, the resultant communicating network is termed as on body, off body and in body WBAN respectively [4]. Out of these networks in body network also termed as In Vivo Body Area Network (In Vivo BAN) is comprised of implantable sensor nodes that aid in real-time monitoring of subjects. Implantable networking technology is a boon for the medical implant sector [5]. In Vivo communication utilizes the human body as a wireless medium for the transmission of the sensed parameters [6]. Implantable nodes may be used for internal health monitoring, cancerous cell detection, internal drug administration, and many more scenarios [7]. Sensed parameters may be transmitted to off body sensor node which finally forwards it to the medical expert to make a timely and accurate diagnosis of the patients. This proves very helpful for the patients who may be living in remote areas or who require 24×7 monitoring [2].

Several implantable sensors have been developed and implemented to monitor specific parameters inside the human body and giving promising results. A detailed study of cardiovascular and other implantable devices has been given in [8]. Different companies have been designing medical implant devices, such as Medtronic Inc., Biotronik Inc., St. Jude Medical, Boston Scientific, and Cameron Health. Zarlink Inc. introduced transceivers for implanted devices such as pacemakers, ICDs, implanted insulin pumps, bladder control monitors, and implantable physiological monitors [9].

Currently, various transmission techniques operating at diverse frequency bands have shown the feasibility of transmitting sensed signals through the human body [10]. Federal Communications Commission (FCC) has proposed Medical Implant Communication Service (MICS) band for implantable communication. This band is quite popular as it offers better

Manuscript received February 16, 2021; revised June 3, 2021; accepted June 5, 2021. Date of publication June 14, 2021; date of current version August 31, 2021. The associate editor coordinating the review of this article and approving it for publication was Prof. Elena Gaura. *(Corresponding author: Sindhu Hak Gupta.)*

Monica Kaushik and Sindhu Hak Gupta are with the Department of Electronics and Communication Engineering, Amity University, Noida 201313, India (e-mail: mkaushik@amity.edu; shak@amity.edu).

Vipin Balyan is with the Department of Electrical, Electronic and Computer Engineering, Cape Peninsula University of Technology, Cape Town 7535, South Africa (e-mail: balyanv@cput.ac.za).

Digital Object Identifier 10.1109/JSEN.2021.3089000

conductivity and less interference in the human body [9]. MICS band (402-405 MHz) is an unlicensed band and segregated by IEEE into channel model CM1 (implant to implant) and CM2 (implant to body surface) as per the scenario in which the sensors may be deployed for measuring the physiological parameters [11]. CM1 works for the implant to implant, it has got certain attributes such as the bandwidth of 300 kHz and supports low data rate operations like heart rate (600bps), blood pressure (1.2Kbps) etc. [12]. MICS band due to bandwidth limitations may not support applications such as medical imaging which require a data rate up to 2.4 Mbps [13]. Industrial, Scientific, Medical (ISM) and Ultra-Wide Band (UWB), etc. have also been incorporated for In Vivo communication. UWB technology is used for transferring information over a wide bandwidth starting at 500 MHz, which is relatively much larger than the MICS band (402– 405 MHz) [14]. ISM and UWB consume high energy which results in a higher depletion rate of battery which is an issue for hardware constrained nodes. Apart from this drawback, these bands are already overloaded with various other applications [15]. These facts make them less suitable for In Vivo communication. In [16] authors have explored the scope of biological applications in terahertz science and stated that a wide range of opportunities are there in the terahertz field. In recent times Terahertz Band (.1THz-10THz) is proving to be a promising solution for In Vivo application because of higher frequency, shorter wavelength, and capture molecular interactions at nanoscale level [17].

The applicability and suitability of terahertz communication in the field of biomedical have been analyzed in [18]. It has been found that the THz band is suitable for nano communication devices within the human body. Higher ranges of terahertz band may be used for optical communication. At optical frequencies, electromagnetic (EM) signals are mainly affected by the scattering losses inside the human body whereas the terahertz band provides envisioned EM nano-communication because of its non-ionization nature for human tissues and is less vulnerable to the propagation effect [19]. The non-ionization nature of terahertz radiation makes it suitable for In Vivo communication as it cannot harm biological tissues inside the body [20]. The impact of terahertz exposure on the internal human tissues has been explored in [21] and the authors stated that there is some temperature increase of human tissue when it is exposed to terahertz radiation. In [22] authors proposed a channel model operating at terahertz band (0.1-10 THz) considering molecular absorption from human tissues and scattering from body particles. In this study authors also investigated the thermal photo effect on cells when exposed to Terahertz radiation and stated that terahertz frequencies could be beneficial for intrabody communication and In Vivo applications. Since the human body offers a wireless medium, information signal sensed by a node may be severely affected due to pathloss incurred and attenuation inside the human body. Characterization of pathloss model inside the human skin at the terahertz range has been proposed in [23], by keeping in account parameters like the number of sweat ducts, the distance between implanted nano nodes and frequency of operation. It has been shown that pathloss is significantly large even for small distances at terahertz frequencies [24]. In this study, the impact of noise on intra-body systems models operating in the THz frequency band has been analyzed. By considering all factors of the noise environment a channel model is proposed by authors for terahertz communication. Study of physical layer authentication scheme for In vivo networks operating in terahertz band has been carried out in [25] and shows a prominent future of secured and authenticated nanonetworks for applications like drug delivery.

Challenges and applicability of implantable WBAN have been discussed in [26] and authors have emphasized that the implantable BANs have a promising future in medicine with consideration of various challenges like energy efficiency, security, bandwidth, etc. Energy is one of the major challenges in WBANs and needs to be investigated exhaustively [27]. The implantable nano sensor nodes may be self-excited or powered by batteries [28]. Self-excited sensors use the human body as the primary energy generator [29] but the main issue is that the energy yield is relatively low [8]. In the case of battery-operated sensor nodes, replacing or recharging these batteries is nearly impossible especially in In Vivo communication. Once the battery gets discharged the node is dead, which makes In Vivo network inefficient [31]. [32] To justify implantation the battery of a sensor node should at least have 12 months of operative lifetime. In traditional implants lifetime of the battery is a maximum of 10 years [33]. When this time has been conceded, the implant might be replaced with another one through the surgery. This will put the patient at risk and overburden him financially [34]. These issues motivated researchers to explore energy-efficient approaches to increase the battery lifetime of implantable sensors to avoid battery replacement and recharging in such challenging scenarios.

In recent years diverse methods and strategies have been proposed to make wireless networks energy efficient. Physical layer protocols [12], MAC protocols [35], maximization of a network lifetime [30], and various energy harvesting (EH) [36] technologies have been proposed and delivered to save energy and extend the lifetime of the sensor node. Cooperative communication signaling is considered a key technology that may improve the performance of wireless networks in terms of power and energy [37]. Cooperative communication offers better energy consumption which in turn extends the battery life of sensors nodes. [38] Multipath fading has an adverse effect on wireless communication, and it has been shown in [39] that cooperative communication can combat the fading effect. In cooperative communication, a statistically independent fading path is provided. More the number of relays more will be the fading paths. Based on the operation performed by relay nodes, cooperative communication may be categorized as Amplify-and-Forward (AF), Decode-and-Forward (DF), and Coded Cooperative Communication [40]. In the In Vivo scenario distance between sensor nodes deployed is comparatively small, under severe fading conditions offered by the wireless nature of the human body, the signal quality deteriorates [41]. Cooperative communication for In Vivo network has been explored lately. The outage probability of a cooperative communication-based In Vivo network has been computed in [42] and it has been stated that there is a 10-fold increase in the performance of the system with cooperative communication. Inside the human body, the propagation medium is heterogeneous as the signal must travel via various human tissues and experiences several losses like molecular and spreading absorption, fading, attenuation, etc. [43]. The performance of a cooperative relaying transmission scheme considering the effect of losses due to spreading and molecular absorption has been studied in [44]. The impact of different human tissues like blood, fat, skin, etc. on the performance of In Vivo cooperative communication has not been explored exhaustively.

To design efficient healthcare communication systems energy efficacy and link quality are some major issues. Link quality is an indication of the quality of data received at the receiver which is an important aspect in healthcare systems as the error in health parameters may lead to severe complications. The link quality can be arbitrated in terms of signal to noise ratio (SNR), bit error rate (BER), etc. [19]. For In Vivo networks the effect of propagation channel on the signal quality is significant hence, mathematical modeling and analysis of the system are desirable for evaluation and analysis of an energy-efficient In Vivo BAN with improved link quality [45]. In literature, different optimization techniques have been suggested to make WBAN an energy-efficient network. But due to the complex nature of the human body, Invivo BAN required efficient optimization techniques that need to be explored thoroughly. The Artificial Neural Network (ANN) practice in the electromagnetics domain is wide [46] and used for optimization purposes in various fields. [47]. Generally, for biomedical data, ANN is a preferred method as it is good in the modeling of nonlinear functions and capable to approximate complex behavior with the desired level of accuracy [53]. The other advantages of the ANN algorithm are its learning abilities, simplicity, fast implementation, flexible modeling, and lower estimated errors [48].

In this work performance of cooperative In Vivo BAN has been investigated under the consideration of the impact of different human tissues. The analysis has been carried out in terms of SNR, received power, and energy for In Vivo BAN. Further optimization of received power and energy have been performed by implementing ANN to the proposed network for making it energy efficient. In this work performance of cooperative In Vivo BAN has been investigated under the consideration of the impact of different human tissues. The analysis has been carried out in terms of SNR, received power, and energy for In Vivo BAN. Further optimization of received power and energy have been performed by implementing ANN to the proposed network for making it energy efficient.

The main contributions of this work are:

- A system model depicting the interrelation between received power, pathloss, SNR, the distance between communicating nodes, antenna gain, and wavelength has been formulated for cooperative as well as non-cooperative In Vivo BAN operating at terahertz band.
- A critical comparative analysis of cooperative and non-cooperative In Vivo BAN operating at terahertz band has been performed considering the effect of different tissues (like fat, skin, water, and blood) existing inside the human body.
- Received power, energy and SNR have been critically examined for the modeled In Vivo BAN.
- Optimization of received power and energy of the modeled network has been carried out using ANN to achieve energy and power efficiency In Vivo BAN operating at terahertz band.

In this work optimization of Invivo BAN using ANN has been performed for energy efficiency. Cooperative approach and different human tissues have been considered as a communication medium for the modelled In Vivo BAN.

In the current work, a system model depicting the interrelation between received power, pathloss, SNR distance between communicating nodes antenna gain and wavelength will be formulated, analyzed, and optimized to achieve an energy-efficient In Vivo network. The rest of the paper is organized as follows, Section II represents related work, In Section III, a system model for In Vivo BAN operating in terahertz band (.5 -10THz) is framed. The optimization of received power and energy using ANN for efficient In Vivo communication is presented in section IV. Section V presents the simulation results of the considered scenarios. Finally, in section VI conclusion of the work is highlighted.

II. Related Work

Various researchers have investigated the use of implantable nanodevices for body area networks. In [4] considering the cooperative scenario, the energy consumption models for a combination of implantable and wearable devices have been presented. BER has been computed and it has been observed that there is a significant energy saving with cooperative strategy. A channel model combining the effect of spreading, scattering and molecular absorption has been proposed in [17] for invivo BAN at terahertz band. A link budget analysis considering the transmit power, pathloss, and receiver sensitivity has been presented by authors and support the practicability of In Vivo BAN at terahertz band. The performance of nanomachines deployed inside the human body has been investigated in [18] and it has been analyzed that human tissues limit the transmission range and suggested a multihop communication strategy to increase the transmission range inside the human body. In [23] a pathloss model operating at terahertz band has been suggested to characterize the communication channel inside the human body. The proposed model consists of different distances, sweat ducts, and frequencies. In [41] cooperative strategies have been presented for In Vivo networks and evaluate the performance of the proposed model in terms of outage probability with respect to transmitted power. The authors stated that using cooperative communication, there is an improvement in the performance of the In-vivo network. Authors in [42] explored the effect of modulation schemes for In Vivo BAN considering different human tissues. Also optimized transmitted power to make In Vivo BAN an energy-efficient BAN.

The cooperative approach for In Vivo BAN considering the impact of human tissues is still needed to be investigated

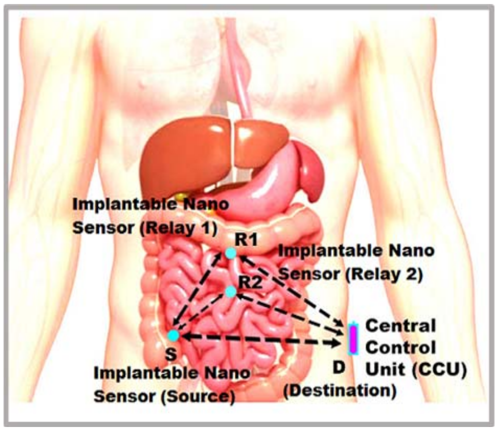

(a)

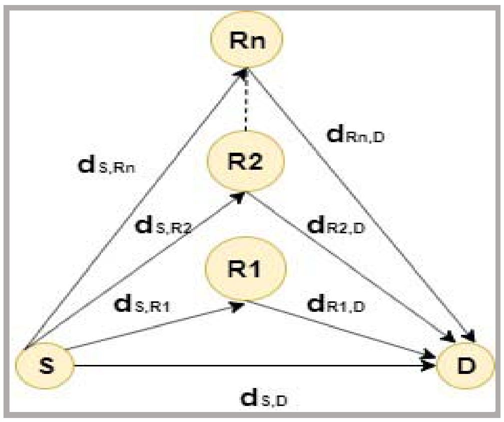

(b)

Fig. 1. Cooperative scenario and relay node placement for in vivo network (a) Cooperative scenario inside the human body (b) Simplified deployment of relay nodes.

exhaustively. As each human tissue has different dielectric properties and impacts the signal quality accordingly. Also, optimization of modeled networks for more efficient In Vivo BANs have not been explored thoroughly. The difference in approach implemented and the metrices evaluated in the current work has been compared with some of the previous work in Table-II given section V.

III. System Model

In Vivo, the sensor-based monitoring system may provide a better approach to evade complications at a later stage such as the relapse of life-threatening disorders. Sensor nodes implanted on or around the sensitive site can sense any change in concerned physiological parameters and transmit to the central control unit. As shown in Fig.1 (a) an In Vivo cooperative network model in which implanted nano sensors are operating at the terahertz band (0.1-10THz) has been assumed. For the modeling of the network, it is assumed that multiple nodes are deployed in the stomach to monitor the physiological parameters pertaining to the detection of cancer symptoms. Suppose node S transmits the sensed parameters to node D which acts as a central control unit (CCU). The node S and node D are separated by the distance $d_{S,D}$. The signal transmitted by node S will be severely affected due to pathloss and fading even propagating to a small distance as seen in the earlier section. This fact will attenuate the signal strength. Since it has been proven that cooperative communication combats the effect of fading, other nodes (R1, R2…. Rn) will act as relay nodes to offer cooperative communication in the said scenario. A simplified version of the deployment of the source node and multiple relay nodes (R1, R2…. Rn) has been shown in Fig.1 (b). For simplicity AF based relaying and only two relay nodes R1 and R2 have been considered. Due to heterogeneous medium, the pathloss is very high in In Vivo communication. By keeping in view, the effect of pathloss on the received signal, for non-cooperative scenario (direct link between the source node and destination node), SNR at the receiver is specified in [46] and given as:

$$\gamma_{S,D} = \frac{|h_{S,D}|^2 \times P_t}{PL_{S,D} \times \sigma^2} \tag{1}$$

where $h_{S,D}$ is complex normally distributed channel gain which is taken unity for simplicity, P_t is the power transmitted by the source node and σ^2 is the variance of additive white Gaussian noise and $PL_{S,D}$ is the pathloss from source node S to destination node D and has been computed in [18] as:

$$PL_{S,D} = -0.2\mathrm{N} + 3.98 + (0.44\mathrm{N} + 98.48)\, d_{S,D}^{.65} + (0.068N + 2.4)\, f^{4.07} \tag{2}$$

Here, f is the operating frequency, $d_{S,D}$ is the distance between the source node and destination node and N is the number of sweat ducts that plays an important role in THz wave interaction with human skin, here N=5

With the help of (1) and (2), SNR at the destination D in the non-cooperative scenario is,

$$\gamma_{S,D} = \frac{|h_{S,D}|^2 \times P_t}{\begin{bmatrix} -0.2\mathrm{N} + 3.98 + (0.44\mathrm{N} + 98.48)\, d_{S,D}^{.65} \\ + (0.068N + 2.4)\, f^{4.07} \end{bmatrix} \times \sigma^2} \tag{3}$$

For the cooperative scenario, multiple relay nodes are used to support communication between the source node and destination node. The received SNR at n^{th} relay node due to connection between the source node (S) and the n^{th} relay node is given by:

$$\gamma_{S,R_n} = \frac{|h_{S,R_n}|^2 P_t}{PL_{S,R_n} \times \sigma^2} \tag{4}$$

Here, P_t is power transmitted by the source node (S) and pathloss due to the link between the source node (S) and n^{th} relay node $PL_{S,Rn}$ can be calculated as:

$$PL_{S,Rn} = -0.2\mathrm{N} + 3.98 + (0.44\mathrm{N} + 98.48)\, d_{S,Rn}^{.65} + (0.068N + 2.4)\, f^{4.07} \tag{5}$$

$d_{S,Rn}$ is the distance between the source node (S) and n^{th} relay node.

From (4) and (5) the SNR at n^{th} relay node can be written as,

$$\gamma_{S,R_n} = \frac{\left|h_{S,R_n}\right|^2 P_t}{\begin{bmatrix} -0.2N + 3.98 + (0.44N + 98.48)\, d_{S,Rn}^{.65} \\ +(0.068N + 2.4)\, f^{4.07} \end{bmatrix} \times \sigma^2} \quad (6)$$

Received SNR($\gamma_{R_n,D}$) and pathloss($PL_{Rn,D}$) at the destination node (D) due to the link between n^{th} relay node and the destination node (D) can be obtained with the help of (1) and (2) respectively. Here unit channel gain and power received at n^{th} relay node is be considered. Distance ($d_{Rn,D}$) is measured from n^{th} relay node to destination. The rest of the parameters will remain same.

Further SNR at destination D can be computed as,

$$\gamma_{R_n,D} = \frac{\left|h_{R_n,D}\right|^2 P_R}{\begin{bmatrix} -0.2\mathrm{N} + 3.98 + (0.44\mathrm{N} + 98.48)\, d_{Rn,D}^{.65} \\ +(0.068N + 2.4)\, f^{4.07} \end{bmatrix} \times \sigma^2} \quad (7)$$

Now as depicted in [25], the total SNR received at the destination node under the cooperative scenario is given as:

$$\gamma_D = \frac{\gamma_{S,Rn}\gamma_{Rn,D}}{\gamma_{S,Rn} + \gamma_{Rn,D} + 1} \quad (8)$$

The value of $\gamma_{S,Rn}$ and $\gamma_{Rn,D}$ can be obtained from (6) and (7).

For Wireless medium, it has been shown in [47] that power received depends on the SNR and data rate (R). On further simplification it may be represented as,

$$\frac{\mathrm{E_b}}{\mathrm{N_0}} = \frac{\mathrm{SNR}}{\mathrm{R}} = \frac{\mathrm{P_r}}{\mathrm{N_0}}\frac{1}{\mathrm{R}} = \frac{1 \times \mathrm{P_t} \times \mathrm{G_t} \times \mathrm{G_r} \times \lambda^2}{\mathrm{N_0} \times R \times (4\pi)^2 \times d_0^{\bar{\gamma}} \times L}\left(\frac{d_0}{d}\right)^{\bar{\gamma}} \quad (9)$$

where $\mathrm{G_t}$ and $\mathrm{G_r}$ are the gain of transmitter and receiver antenna respectively, $\bar{\gamma}$ is the pathloss exponent, R is the data rate, $\mathrm{P_t}$ is the power transmitted by source node and $\mathrm{E_b/N_0}$ is the ratio of energy per bit and noise level, SNR is signal to noise ratio. d is the separation distance between the source node and destination node in mm and $\mathrm{d_0}$ is the reference distance in mm.

For the considered scenario, with the help of (9), the received power at n^{th} relay node ($P_{r_{R_n}}$) can be expressed as,

$$P_{r_{R_n}} = \frac{\gamma_{S,Rn} \times N_0 \times G_t \times G_r \times \left(\frac{c}{\sqrt{\varepsilon \times f}}\right)^2}{(4\pi)^2 \times d_{s,R}^{\bar{\gamma}} \times PL_{S,Rn}} \quad (10)$$

Similarly, the power received at the destination can be written as,

$$P_{r_D} = \frac{\gamma_{Rn,D} \times N_0 \times G_t \times G_r \times \left(\frac{c}{\sqrt{\varepsilon \times \mathrm{f}}}\right)^2}{(4\pi)^2 \times d_{R,,D}^{\bar{\gamma}} \times PL_{Rn,D}} \quad (11)$$

It is evident from (11) that received power P_{r_D} at the destination node is a function of SNR ($\gamma_{Rn,D}$), noise figure ($\mathrm{N_0}$), gain of transmitting ($\mathrm{G_t}$) and receiving antenna ($\mathrm{G_r}$), the permittivity of human tissues (ε), speed of light (c), operating frequency(f), the distance between communicating nodes ($\mathrm{d_{R,D}}$), pathloss exponent ($\bar{\gamma}$), and pathloss ($PL_{Rn,D}$). Out of these parameters pathloss exponent, speed of light, the permittivity of human tissues and noise figure are constrained parameters whereas SNR, antenna gain ($\mathrm{G_t}$, $\mathrm{G_r}$) distance ($\mathrm{d_{R,D}}$), and pathloss ($PL_{Rn,D}$) are free parameters and nonlinear in nature. Free parameters can be optimized to attain an energy-efficient In Vivo BAN. In the subsequent section optimization of the free parameters has been carried out using ANN.

IV. Optimization

A. Formulation

Optimization of SNR to find the efficient value of received power and energy for In Vivo network operating at terahertz band by applying ANN using neural network fitting tool.

ANN is used for modeling nonlinear functions and to optimize received power and energy for proposed In Vivo BAN. From equation (11) SNR can be obtained as,

$$\gamma_{Rn,D} = \frac{P_{r_D} \times (4\pi)^2 \times d_{R,,D}^{\bar{\gamma}} \times PL_{Rn,D}}{N_0 \times G_t \times G_r \times \left(\frac{c}{\sqrt{\varepsilon} \times f}\right)^2} \quad (12)$$

It has been observed in (12) that SNR ($\gamma_{\mathrm{Rn,D}}$) depends upon the various parameters like the received power, the distance between communicating node, pathloss, antenna gain, the permittivity of human tissues, frequency, noise figure, pathloss exponent, and speed of light. SNR is directly proportional to some of the parameters like received power, distance and pathloss) whereas having an inverse relationship with antenna gain and other parameters. SNR in (12) is observed to be a non-linear function and has been considered as an objective function to perform optimization using the ANN tool. The considered set up has only 3 parameters in the input space and needs a regression model. The Scaled Conjugate Gradient (SCG) algorithm is the most efficient training algorithm as it updates weight and bias values according to the scaled conjugate gradient method. In the SCG algorithm, the step size is a function of quadratic approximation of the error function [53]. Considering having an initial parameter vector $\mathrm{u_0}$ and an initial training direction vector $\mathrm{j_o} = -\mathrm{k_0}$, the training directions can be created as given in [54],

$$j_{i+1} = k_{i+1} + j_i X_i, \quad i = 0, 1, 2, 3 \ldots\ldots \quad (13)$$

Here, j is the training direction vector, X is the conjugate parameter. In SCG, the training direction is always reset to negative of the gradient. The next expression [54] shows how the weights of the neural network can be updated,

$$u_{i+1} = u_i + d_i r_i, \quad i = 0, 1, 2, 3, \ldots. \quad (14)$$

SCG algorithm has been implemented to train ANN for this work, using the neural network toolbox of MATLAB [52]. ANN model used for this work consists of three layers: an input layer, output layer, and a hidden layer, as shown in Fig. 2. A data set of approximated 5000 samples of SNR, pathloss has been created for cooperative and non-cooperative scenarios considering different human tissues (skin, blood, water, and fat) using the mathematical model expressed in (12). The number of neurons in the hidden layer has been

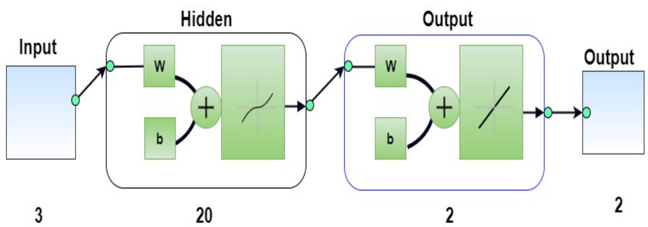

Fig. 2. Neural network training model for optimization [53].

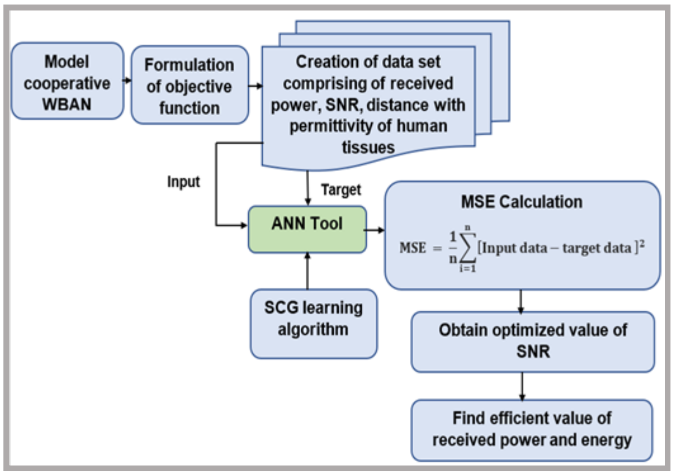

Fig. 3. Flow graph of proposed solution.

TABLE I
SIMULATION PARAMETERS

Parameters	Value	Ref.
Transmitted Power	100nW	[21]
Noise Figure (N_0)	-174 dBm	[21]
Data Rate	25 Gbps	[17]
Pathloss exponent	3.5	[13]

chosen carefully to avoid issues like underfitting, overfitting, and an increase in training time of the network. The input layer consists of 3 parameters namely pathloss, distance, received power according to the different human tissues and SNR is used as the target parameter. For this analysis, the created data set is randomly divided into three parts: 80 % of data is used for training, and 10 % each is used for testing and validation respectively. This is the standard and most common distribution of data for training, testing, and validation in ANN to prevent overfitting. The goal of optimization is to find a value of SNR which is the best among the total number of samples. The performance of the neural network has been evaluated using Mean Square Error (MSE) function (loss/cost function) and regression analysis. The function is expressed as the sum of the squared differences, between the target value and input. The mathematical evaluation of MSE is given in [49] and for the current scenario it is represented in (15)

$$\text{MSE of SNR} = \frac{1}{n}\sum_{i=1}^{n}\left[\text{Input data} - \text{target(SNR)}\right]^2 \quad (15)$$

Here n= total number of data samples.

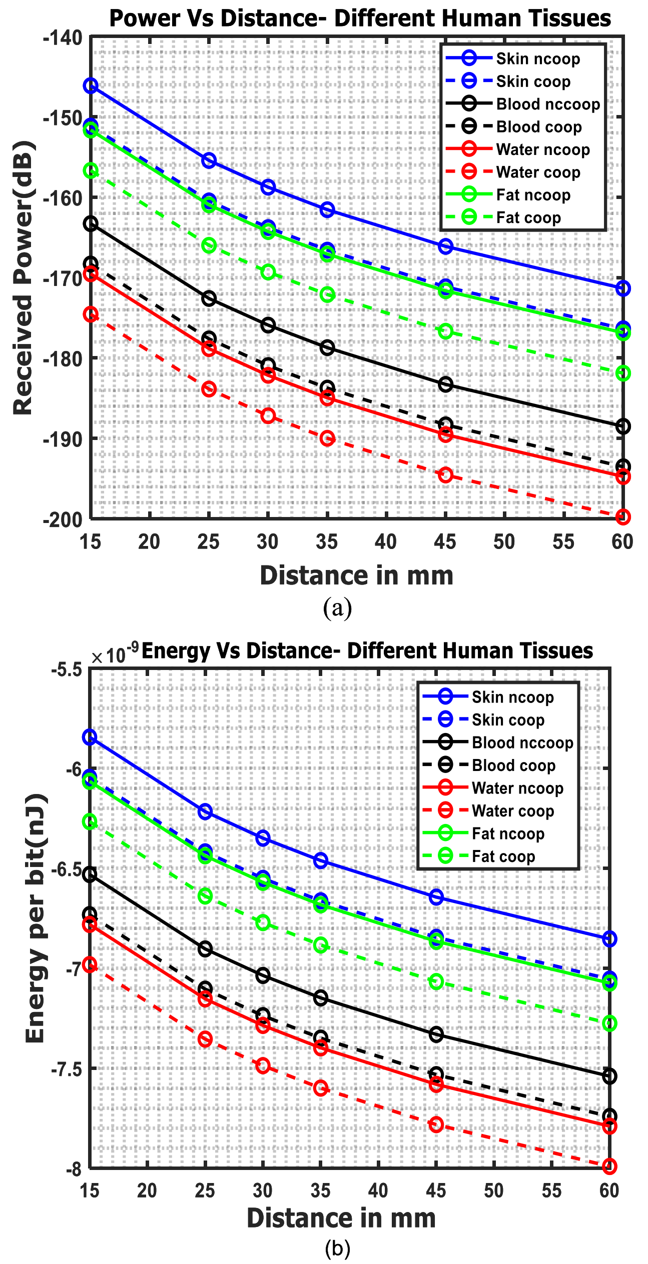

Fig. 4. Received power and energy impacted by human tissues in cooperative and non-cooperative in vivo scenario (a) received power with distance (b) received energy with distance.

Utilizing SCG algorithm, the mean square error (MSE) function has been calculated and used to obtain the optimized value of SNR which is further used to find the efficient value of received power and energy for the In Vivo BAN. The training process terminates if the error function is minimized or the number of predefined iterations has been passed. The optimized SNR is further used to elevate the network performance in terms of received energy and power for the considered scenario. Flow graph of proposed work has been shown in Fig.3 The next section portrays the performance analysis of the proposed model with the help of simulation results.

V. RESULTS AND DISCUSSION

To analyze the performance of cooperative as well as non-cooperative In Vivo BAN operating at 1 THz frequency the

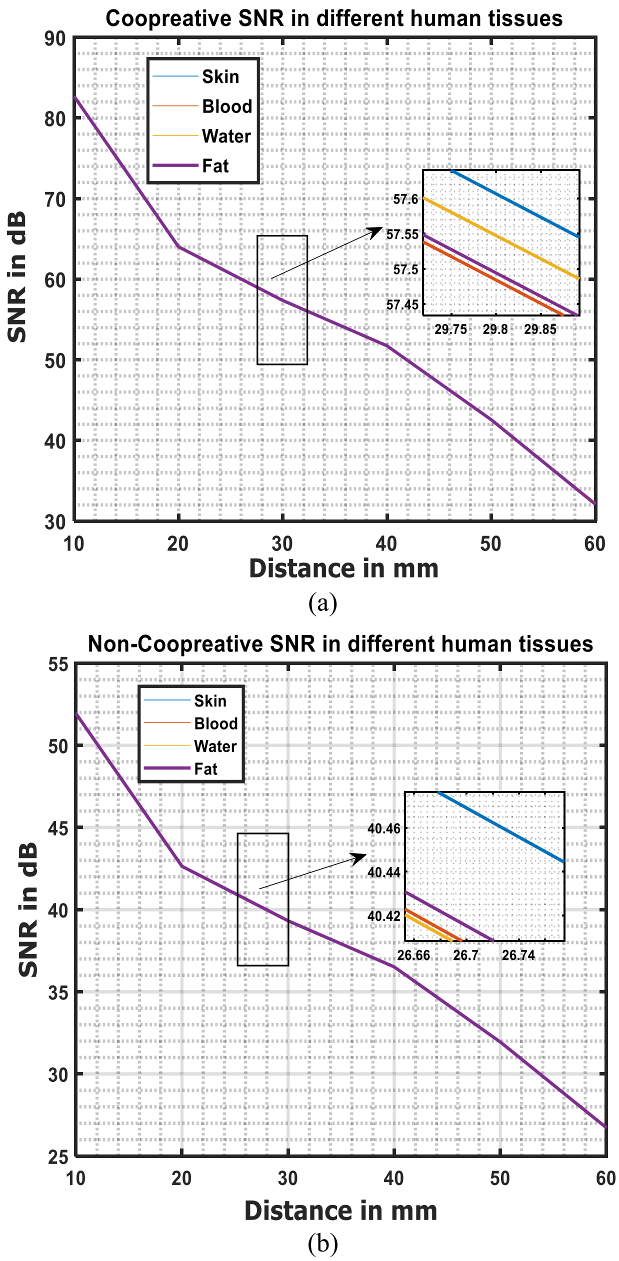

Fig. 5. SNR impacted by human tissues in invivo BAN scenario (a) cooperative SNR with distance and (b) non-cooperative with distance.

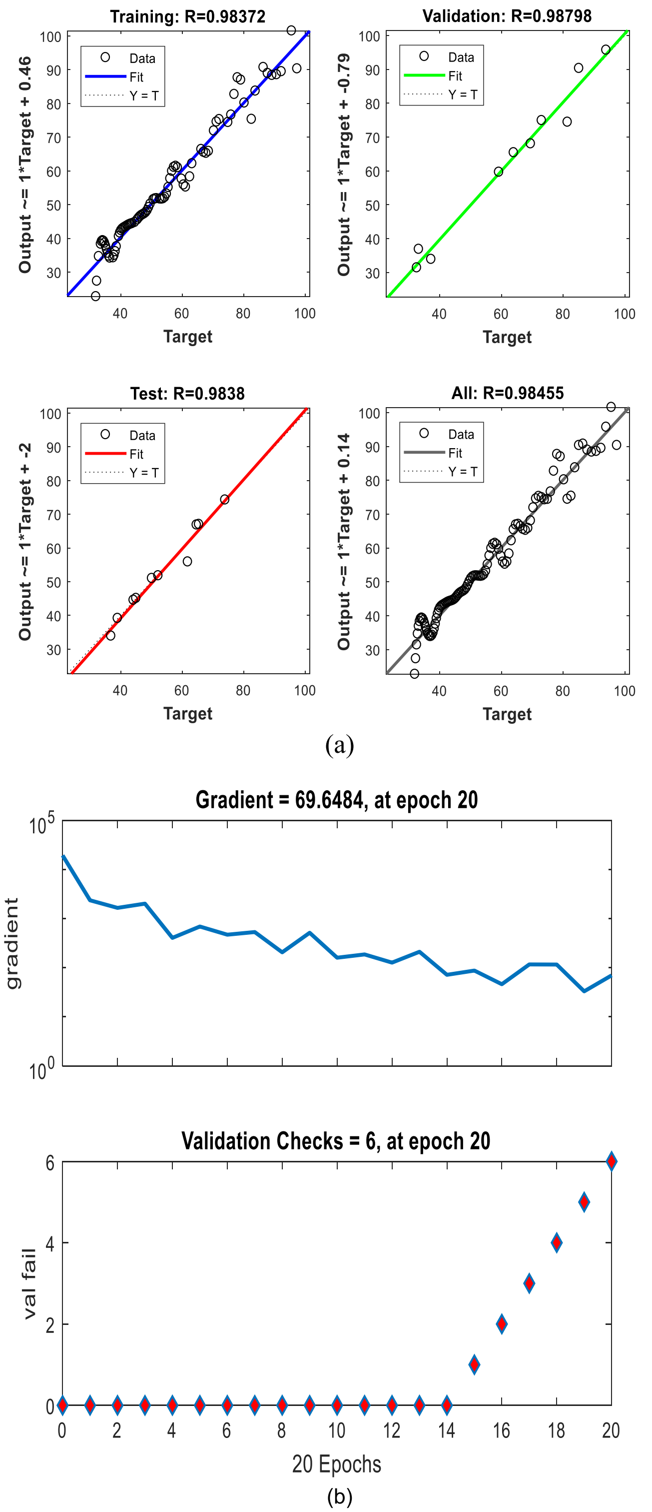

Fig. 6. Regression and validation plot of ANN model (a) Regression plots for training, testing, and validation (b) performance variation of gradient error and validation checks.

considered scenario is shown in Fig.1. For current work the permittivity (ε) of blood, skin, water, and fat at 1 THz is taken as 0.5130, 0.2625,.7062, 0.1910 respectively [16]. Parameters used for simulation has been given in Table-I.

A comparative analysis of cooperative and non-cooperative In Vivo BAN under the consideration of human tissues (skin, blood, water, and fat) is presented in Fig.4. As observed from Fig.4 (a) and 4(b), under cooperative scenario, In Vivo BAN shows a remarkable improvement in received power and energy in comparison to a non-cooperative scenario. A critical comparative analysis of cooperative and non-cooperative scenarios exhibits that received power is approximately increased by 16% in cooperative communication. It may be stated that for In Vivo communication skin offers the least attenuation in the propagated signal in comparison to the blood, fat, and water. Further, it is observed that cooperative communication improves the performance of In Vivo BAN. As mentioned above different human tissues have different permittivity which significantly impacts the quality of propagated signal which

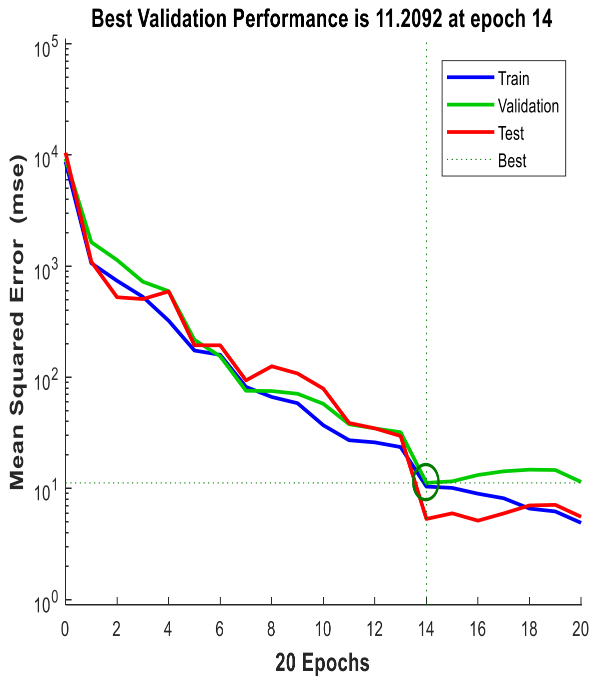

(a)

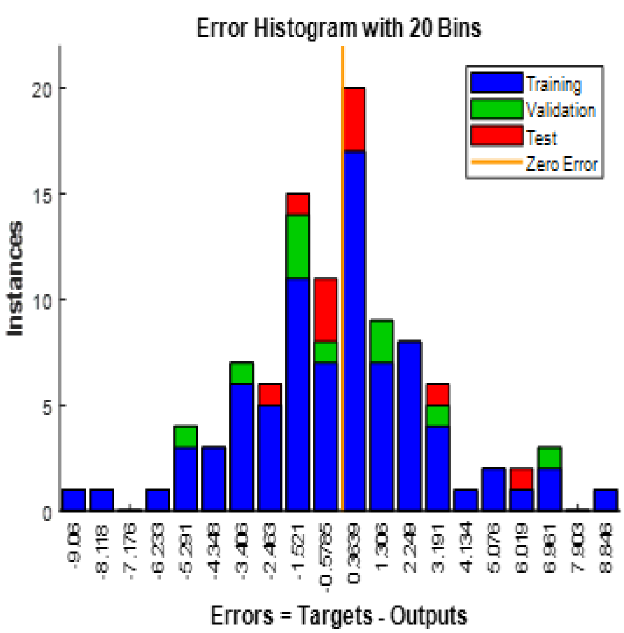

(b)

Fig. 7. Performance of ANN model (a) best validation (b) Error Histogram.

can be measured in terms of SNR. Higher SNR reflects good quality of the received signal. A comparative analysis of cooperative and non-cooperative SNR considering different human tissues has been shown in Fig.5(a) and Fig.5(b). SNR is linearly decreasing with an increase in distance. There

TABLE II
COMPARATIVE TABLE OF RELATED WORK

	Human Tissues	Approach	WBAN Type	Matrices Evaluated	Optimized
[4]	×	C	On-Off Body	BER, Energy Consumption	×
[17]	✓	NC	In Vivo	Pathloss Transmit Power Receiver Sensitivity	×
[18]	✓	C	In Vivo	Transmission range Channel Capacity	×
[22]	✓	NC	In Vivo	Molecular absorption Thermal Photo effect	×
[23]	✓	NC	In Vivo	Pathloss	×
[42	✓	C	In Vivo	Outage Probability Transmit Power	×
[43]	✓	NC	In Vivo	Pathloss Modulation Schemes Transmitted Power	✓
current Work	✓	C	In Vivo	SNR Received Power Received Energy	✓

*C= Cooperative and NC= Non-Cooperative

is minimal difference in SNR for different human tissues (approximately.01%). The variation in SNR has been highlighted by the inset subplot in the graph. The cooperative scenario shows marginal improvement in SNR in comparison to non-cooperative scenario.

As discussed earlier a data set has been created by taking various human tissues (skin, blood, fat, and water) into account. The impact of all tissues has been studied analytically and it has been observed that skin is the best propagation medium for In Vivo communication. Keeping this in view ANN has been implemented for optimization considering the data set created by taking skin as the base muscle with its associated permittivity.

Fig.6 and Fig.7 represents the performance plots of ANN model. Fig 6 (a) represents the regression curve fit for the input and output data set. The regression plots show the output with respect to targets for training, validation, and

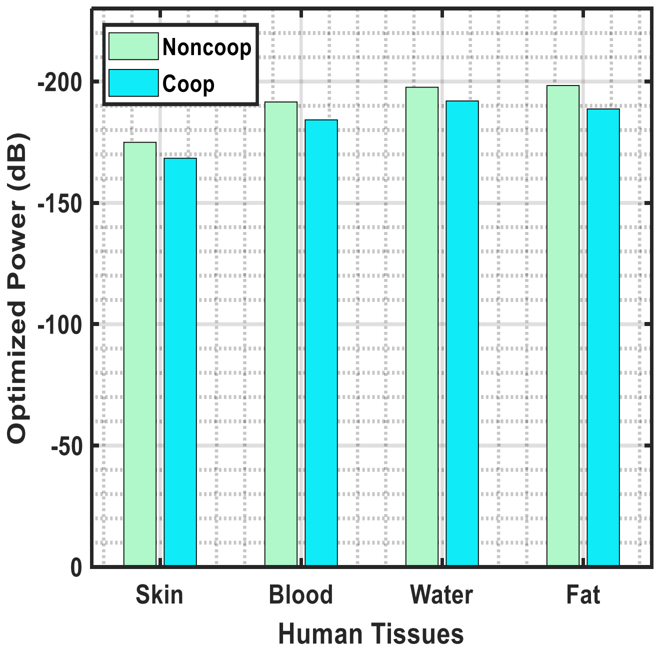

(a)

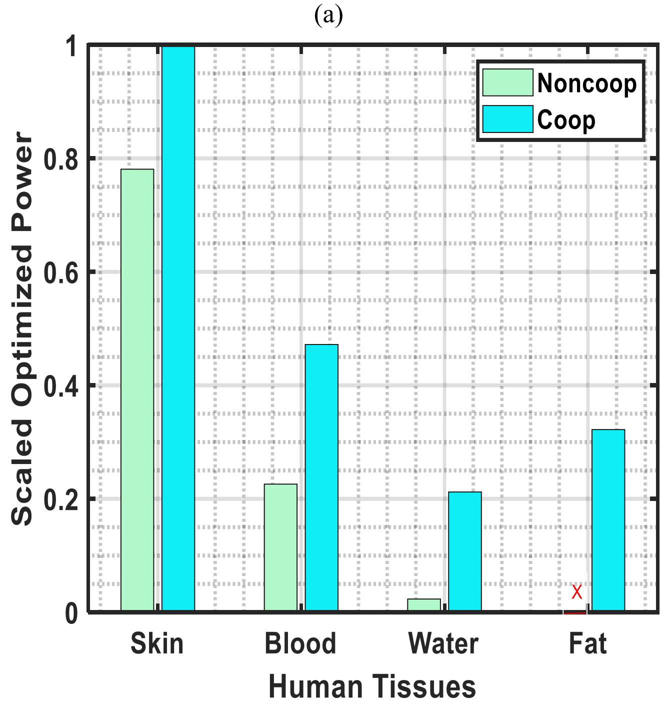

(b)

Fig. 8. Comparative plot (a) Optimized power for different human tissues in cooperative and non-cooperative in vivo scenario (b) Scaled optimized power.

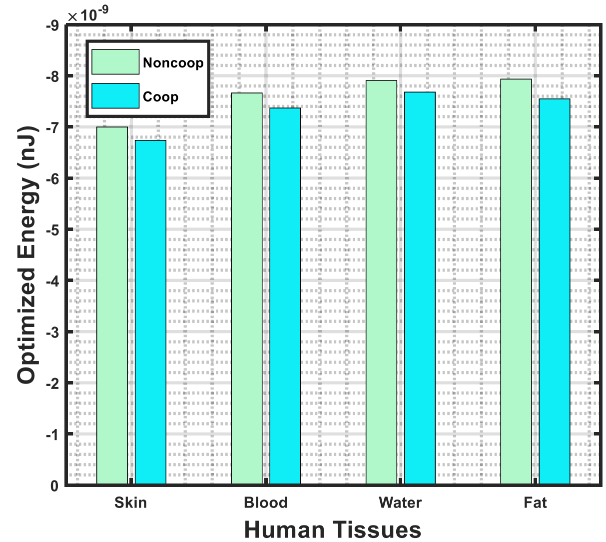

(a)

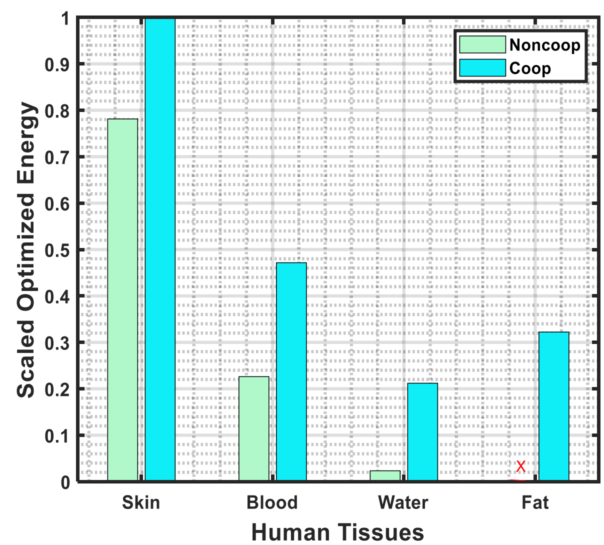

(b)

Fig. 9. Comparative plot (a) Optimized energy for different human tissues in cooperative non-cooperative in vivo scenario (b) Scaled optimized energy.

test sets. The dashed line represents the perfect result that is Output (Y) = Targets (T) and R value indicate the relationship between output and target. Here the curve fit is just good for all data sets, as R values in each result are 0.98 it means 98% accuracy. Fig. 6(b) depicts the values of the gradient and validation check. At epoch 20 gradient and validation checks are 69.6484 and 6 respectively. In Fig 7(a) the system performance is analyzed in terms of the number of epochs versus Mean Square Error (MSE). The graph indicates that the MSE decreases with the increase in the number of epochs for all trained, validation, and test data with a small variation. For a well-trained ANN, target outputs and the ANN's outputs for the training set should be very near to each other. Here at epoch 14 output for the training set gives the best validation. For further verification of the performance error histogram for the ANN model is shown in Fig.7(b). Errors are mostly distributed between -6.233 and 6.961. Though, the maximum errors for training and testing data points are -.9.06 and 8.846, respectively, in comparison to the rest of the dataset errors The minimum error value of SNR (23.94908 dB) is obtained which is further used to optimize received power and energy training and testing data points are -.9.06 and 8.846, respectively, in comparison to the rest of the dataset errors.

The sensors used in In Vivo BANs are battery constraints. It is not feasible to replace or recharge the battery. Therefore, power and energy optimization is required to make In Vivo BAN an energy efficient network. Fig.8 and Fig.9 show a comparative analysis of optimized power and energy for cooperative and non-cooperative scenarios respectively. The impact of human tissue has also been considered for the same.

The results indicate that the performance of cooperative scenario is better than the non-cooperative scenario as in cooperative scenario optimized received power and energy are higher. For the skin tissue as communicating medium, there is approximately 22% increase in received power and approximately 96% increase in received energy. Apart from skin, for blood, fat and water tissues as communicating medium cooperative communication also shows improvement in received power in comparison to non-cooperative approach by 18%, 10.7% and 27% respectively. Similarly, cooperative communication depicts increment in energy for blood, fat and water tissues by 96%, 95% and 97% respectively in comparison to non-cooperative scenario. For more clear and Fig.9(b) respectively for cooperative and non-cooperative presentation the scaled optimized received power and energy given in Fig. 8 (b) scenarios. Normalization aims to scale the data within a fixed range varying from 0 to 1 without disturbing the differences in the range of actual evaluated values. Normalization of data is achieved by subtracting the instantaneous data value from the minimum value in the data set and dividing the resultant value by the difference of maximum and minimum value from data set. In the next section conclusion of the current work has been highlighted.

VI. Conclusion

In the current work, a critical comparative analysis of cooperative and non-cooperative In Vivo sensor networks in terms of received power and energy has been carried out at terahertz frequency. The impact of different human tissues such as skin, blood, fat, and water on the received power as well as energy has been analyzed for In Vivo sensor network. Terahertz band has been chosen as it is not harmful to human tissues. In order to compute received power and energy, a mathematical model for cooperative and non-cooperative In Vivo sensor networks with various parameters such as pathloss, distance, the permittivity of human tissues has been formulated. A data set with 5000 samples of pathloss, distance and other valid parameters have been created. ANN is implemented for optimization and the minimum error value of SNR is obtained which is further used to get optimized received power and energy. Results reveal that the performance of cooperative communication is better than the non-cooperative communication in In Vivo network. Simulation results show that the performance of the cooperative In Vivo sensor network is promising in comparison to non-cooperative In Vivo sensor network. Under cooperative scenario, there is approx. 22% increase in received power in the skin, 18%, in blood, 27% in water and 11% in fat, and average 75 % increase in received energy in comparison to the non-cooperative In Vivo network. Skin seems the best medium in comparison to other human tissues for cooperative as well as non-cooperative scenario as received power and energy is maximum in the skin. After optimization, received power is increased by 37 % and 49 % for the non-cooperative and cooperative scenario respectively and energy is increased by 11% and 20% for non-cooperative and cooperative scenarios respectively. Along with numerous benefits, there are certain challenges associated with In Vivo BANs like sensor deployment, real-time analysis, and correct selection of operating frequency. Exhaustive experimental study and evaluation are required to ensure that the operating frequency like MICS band (402-405MHz), THz band (.3-3 THz) on which In vivo band operates do not induce a thermal effect on human tissues.

References

[1] C. Yi, L. Wang, and Y. Li, "Energy efficient transmission approach for WBAN based on threshold distance," *IEEE Sensors J.*, vol. 15, no. 9, pp. 5133–5141, Sep. 2015, doi: 10.1109/JSEN.2015.2435814.

[2] S. C. Mukhopadhyay, "Wearable sensors for human activity monitoring: A review," *IEEE Sensors J.*, vol. 15, no. 3, pp. 1321–1330, Mar. 2015, doi: 10.1109/JSEN.2014.2370945.

[3] J. Park, "Bio-inspired approach for inter-WBAN coexistence," *IEEE Trans. Veh. Technol.*, vol. 68, no. 7, pp. 7236–7240, Jul. 2019, doi: 10.1109/TVT.2019.2917915.

[4] Y. Peng and L. Peng, "A cooperative transmission strategy for body-area networks in healthcare systems," *IEEE Access*, vol. 4, pp. 9155–9162, 2016, doi: 10.1109/ACCESS.2016.2635695.

[5] B. Latré, B. Braem, I. Moerman, C. Blondia, and P. Demeester, "A survey on wireless body area networks," *Wireless Netw.*, vol. 17, no. 1, pp. 1–18, Jan. 2011, doi: 10.1007/s11276-010-0252-4.

[6] A. F. Demir *et al.*, "Anatomical region-specific *in vivo* wireless communication channel characterization," *IEEE J. Biomed. Health Informat.*, vol. 21, no. 5, pp. 1254–1262, Sep. 2017, doi: 10.1109/JBHI.2016.2618890.

[7] A. Trigui, S. Hached, A. C. Ammari, Y. Savaria, and M. Sawan, "Maximizing data transmission rate for implantable devices over a single inductive link: Methodological review," *IEEE Rev. Biomed. Eng.*, vol. 12, pp. 72–87, 2019, doi: 10.1109/RBME.2018.2873817.

[8] A. Bussooa, S. Neale, and J. Mercer, "Future of smart cardiovascular implants," *Sensors*, vol. 18, no. 7, p. 2008, Jun. 2018, doi: 10.3390/s18072008.

[9] M. N. Islam and M. R. Yuce, "Review of medical implant communication system (MICS) band and network," *ICT Exp.*, vol. 2, no. 4, pp. 188–194, Dec. 2016, doi: 10.1016/j.icte.2016.08.010.

[10] I. F. Akyildiz and J. M. Jornet, "Electromagnetic wireless nanosensor networks," *Nano Commun. Netw.*, vol. 1, no. 1, pp. 3–19, 2010, doi: 10.1016/j.nancom.2010.04.001.

[11] K. Yazdandoost and K. Sayrafian, *Channel Model for Body Area Network (BAN)*, IEEE Standard P802.15-08-0780-09-0006, IEEE 802.15 Working Group Document, 2009.

[12] J. Abouei, J. D. Brown, K. N. Plataniotis, and S. Pasupathy, "Energy efficiency and reliability in wireless biomedical implant systems," *IEEE Trans. Inf. Technol. Biomed.*, vol. 15, no. 3, pp. 456–466, May 2011, doi: 10.1109/TITB.2011.2105497.

[13] FCC, Washington, DC, USA. (Mar. 2003). *Code of Federal Regulations (CFR), MICS Band Plan*. [Online]. Available: http://www.fcc.gov

[14] M. Ilyas, O. N. Ucan, O. Bayat, X. Yang, and Q. H. Abbasi, "Mathematical modeling of ultra wideband *in vivo* radio channel," *IEEE Access*, vol. 6, pp. 20848–20854, 2018, doi: 10.1109/ACCESS.2018.2823741.

[15] J. M. Jornet and I. F. Akyildiz, "Channel modeling and capacity analysis for electromagnetic wireless nanonetworks in the terahertz band," *IEEE Trans. Wireless Commun.*, vol. 10, no. 10, pp. 3211–3221, Oct. 2011, doi: 10.1109/TWC.2011.081011.100545.

[16] A. R. Orlando and G. P. Gallerano, "Terahertz radiation effects and biological applications," *J. Infr., Millim., THz Waves*, vol. 30, pp. 1308–1318, Aug. 2009, doi: 10.1007/s10762-009-9561-z.

[17] M. O. Iqbal, M. M. Ur Rahman, M. A. Imran, A. Alomainy, and Q. H. Abbasi, "Modulation mode detection and classification for *in vivo* nano-scale communication systems operating in terahertz band," *IEEE Trans. Nanobiosci.*, vol. 18, no. 1, pp. 10–17, Jan. 2019, doi: 10.1109/TNB.2018.2882063.

[18] H. Elayan, R. M. Shubair, J. M. Jornet, and P. Johari, "Terahertz channel model and link budget analysis for intrabody nanoscale communication," *IEEE Trans. Nanobiosci.*, vol. 16, no. 6, pp. 491–503, Sep. 2017, doi: 10.1109/TNB.2017.2718967.

[19] G. Piro, K. Yang, G. Boggia, N. Chopra, L. A. Grieco, and A. Alomainy, "Terahertz communications in human tissues at the nanoscale for healthcare applications," *IEEE Trans. Nanotechnol.*, vol. 14, no. 3, pp. 404–406, May 2015, doi: 10.1109/TNANO.2015.2415557.

[20] H. Guo, P. Johari, J. M. Jornet, and Z. Sun, "Intra-body optical channel modeling for *in vivo* wireless nanosensor networks," *IEEE Trans. Nanobiosci.*, vol. 15, no. 1, pp. 41–52, Jan. 2016, doi: 10.1109/TNB.2015.2508042.

[21] O. Spathmann *et al.*, "Thermal impact on the human oral cavity exposed to radiation from biomedical devices operating in the terahertz frequency range," *J. Infr., Millim., Terahertz Waves*, vol. 39, no. 9, pp. 926–941, Sep. 2018, doi: 10.1007/s10762-018-0511-5.

[22] H. Elayan, R. M. Shubair, and J. M. Jornet, "Characterising THz propagation and intrabody thermal absorption in iWNSNs," *IET Microw., Antennas Propag.*, vol. 12, no. 4, pp. 525–532, Mar. 2018, doi: 10.1049/iet-map.2017.0603.

[23] Q. H. Abbasi, H. El Sallabi, N. Chopra, K. Yang, K. A. Qaraqe, and A. Alomainy, "Terahertz channel characterization inside the human skin for nano-scale body-centric networks," *IEEE Trans. THz Sci. Technol.*, vol. 6, no. 3, pp. 427–434, May 2016, doi: 10.1109/TTHZ.2016.2542213.

[24] H. Elayan, C. Stefanini, R. M. Shubair, and J. M. Jornet, "End-to-end noise model for intra-body terahertz nanoscale communication," *IEEE Trans. Nanobiosci.*, vol. 17, no. 4, pp. 464–473, Oct. 2018, doi: 10.1109/TNB.2018.2869124.

[25] M. M. U. Rahman, Q. H. Abbasi, N. Chopra, K. Qaraqe, and A. Alomainy, "Physical layer authentication in nano networks at terahertz frequencies for biomedical applications," *IEEE Access*, vol. 5, pp. 7808–7815, 2017, doi: 10.1109/ACCESS.2017.2700330.

[26] A. Darwish and A. E. Hassanien, "Wearable and implantable wireless sensor network solutions for healthcare monitoring," *Sensors*, vol. 11, no. 6, pp. 5561–5595, May 2011, doi: 10.3390/s110605561.

[27] R. Prakash, A. B. Ganesh, and S. V. Girish, "Cooperative wireless network control based health and activity monitoring system," *J. Med. Syst.*, vol. 40, no. 10, p. 216, Oct. 2016, doi: 10.1007/s10916-016-0576-4.

[28] H. Moosavi and F. M. Bui, "Delay-aware optimization of physical layer security in multi-hop wireless body area networks," *IEEE Trans. Inf. Forensics Security*, vol. 11, no. 9, pp. 1928–1939, Sep. 2016, doi: 10.1109/TIFS.2016.2566446.

[29] V. Bhatnagar and P. Owende, "Energy harvesting for assistive and mobile applications," *Energy Sci. Eng.*, vol. 3, no. 3, pp. 153–173, May 2015, doi: 10.1002/ese3.63.

[30] H. Yetgin, K. T. K. Cheung, M. El-Hajjar, and L. Hanzo, "A survey of network lifetime maximization techniques in wireless sensor networks," *IEEE Commun. Surveys Tuts.*, vol. 19, no. 2, pp. 828–854, 2nd Quart., 2017, doi: 10.1109/COMST.2017.2650979.

[31] I. Caragiannis, C. Kaklamanis, and P. Kanellopoulos, "Energy-efficient wireless network design," *Theory Comput. Syst.*, vol. 39, no. 5, pp. 593–617, Sep. 2006, doi: 10.1007/s00224-005-1204-8.

[32] P. Valdastri, E. Susilo, T. Forster, C. Strohhofer, A. Menciassi, and P. Dario, "Wireless implantable electronic platform for chronic fluorescent-based biosensors," *IEEE Trans. Biomed. Eng.*, vol. 58, no. 6, pp. 1846–1854, Jun. 2011, doi: 10.1109/TBME.2011.2123098.

[33] G. Xu, X. Yang, Q. Yang, J. Zhao, and Y. Li, "Design on magnetic coupling resonance wireless energy transmission and monitoring system for implanted devices," *IEEE Trans. Appl. Supercond.*, vol. 26, no. 4, pp. 1–4, Jun. 2016.

[34] N. Yin *et al.*, "Analysis of wireless energy transmission for implantable device based on coupled magnetic resonance," *IEEE Trans. Magn.*, vol. 48, no. 2, pp. 723–726, Feb. 2012, doi: 10.1109/TMAG.2011.2174341.

[35] D. A. Hammood *et al.*, "Enhancement of the duty cycle cooperative medium access control for wireless body area networks," *IEEE Access*, vol. 7, pp. 3348–3359, 2019, doi: 10.1109/ACCESS.2018.2886291.

[36] D. Rozgic and D. Markovic, "A miniaturized 0.78-mW/cm^2 autonomous thermoelectric energy-harvesting platform for biomedical sensors," *IEEE Trans. Biomed. Circuits Syst.*, vol. 11, no. 4, pp. 773–783, Aug. 2017, doi: 10.1109/TBCAS.2017.2684818.

[37] Y. Chen *et al.*, "Cooperative communications in ultra-wideband wireless body area networks: Channel modeling and system diversity analysis," *IEEE J. Sel. Areas Commun.*, vol. 27, no. 1, pp. 5–16, Jan. 2009, doi: 10.1109/JSAC.2009.090102.

[38] M. Effatparvar, M. Dehghan, and A. M. Rahmani, "A comprehensive survey of energy-aware routing protocols in wireless body area sensor networks," *J. Med. Syst.*, vol. 40, no. 9, p. 201, Sep. 2016, doi: 10.1007/s10916-016-0556-8.

[39] M. Cheffena, "Performance evaluation of wireless body sensors in the presence of slow and fast fading effects," *IEEE Sensors J.*, vol. 15, no. 10, pp. 5518–5526, Oct. 2015, doi: 10.1109/JSEN.2015.2443251.

[40] L. C. Tran, A. Mertins, X. Huang, and F. Safaei, "Comprehensive performance analysis of fully cooperative communication in WBANs," *IEEE Access*, vol. 4, pp. 8737–8756, 2016, doi: 10.1109/ACCESS.2016.2637568.

[41] F. Dressler and S. Fischer, "Connecting in-body nano communication with body area networks: Challenges and opportunities of the Internet of nano things," *Nano Commun. Netw.*, vol. 6, no. 2, pp. 29–38, Jun. 2015, doi: 10.1016/j.nancom.2015.01.006.

[42] Q. H. Abbasi, A. A. Nasir, K. Yang, K. A. Qaraqe, and A. Alomainy, "Cooperative *in-vivo* nano-network communication at terahertz frequencies," *IEEE Access*, vol. 5, pp. 8642–8647, 2017, doi: 10.1109/ACCESS.2017.2677498.

[43] M. Kaushik, S. H. Gupta, and V. Balyan, "Power optimization of invivo sensor node operating at terahertz band using PSO," *Optik*, vol. 202, Feb. 2020, Art. no. 163530, doi: 10.1016/j.ijleo.2019.163530.

[44] N. Chopra, K. Yang, Q. H. Abbasi, K. A. Qaraqe, M. Philpott, and A. Alomainy, "THz time-domain spectroscopy of human skin tissue for in-body nanonetworks," *IEEE Trans. THz Sci. Technol.*, vol. 6, no. 6, pp. 803–809, Nov. 2016, doi: 10.1109/TTHZ.2016.2599075.

[45] Z. Rong, M. S. Leeson, and M. D. Higgins, "Relay-assisted nanoscale communication in the THz band," *Micro Nano Lett.*, vol. 12, no. 6, pp. 373–376, Jun. 2017, doi: 10.1049/mnl.2017.0016.

[46] H. Moosavi and F. M. Bui, "Optimal relay selection and power control with quality-of-service provisioning in wireless body area networks," *IEEE Trans. Wireless Commun.*, vol. 15, no. 8, pp. 5497–5510, Aug. 2016, doi: 10.1109/TWC.2016.2560820.

[47] C. Christodoulou and M. Georgiopoulos, *Applications of Neural Networks in Electromagnetics*. Norwood, MA, USA: Artech House, 2000.

[48] S. P. Sotiroudis, S. K. Goudos, K. A. Gotsis, K. Siakavara, and J. N. Sahalos, "Application of a composite differential evolution algorithm in optimal neural network design for propagation path-loss prediction in mobile communication systems," *IEEE Antennas Wireless Propag. Lett.*, vol. 12, pp. 364–367, 2013, doi: 10.1109/LAWP.2013.2251994.

[49] N. Irfan, M. Bolic, M. C. E. Yagoub, and V. Narasimhan, "Neural-based approach for localization of sensors in indoor environment," *Telecommun. Syst.*, vol. 44, nos. 1–2, pp. 149–158, Jun. 2010, doi: 10.1007/s11235-009-9223-4.

[50] C. G. Siontorou, G.-P. D. Nikoleli, D. P. Nikolelis, S. Karapetis, N. Tzamtzis, and S. Bratakou, "Point-of-care and implantable biosensors in cancer research and diagnosis," in *Next Generation Point-of-Care Biomedical Sensors Technologies for Cancer Diagnosis*. Singapore: Springer, 2017, pp. 115–132, doi: 10.1007/978-981-10-4726-8_5.

[51] J. G. Proakis, *Digital Communications*, 4th ed. Boston, MA, USA: McGraw-Hill, 2001, p. 7.

[52] S. K. Goudos, G. V. Tsoulos, G. Athanasiadou, M. C. Batistatos, D. Zarbouti, and K. E. Psannis, "Artificial neural network optimal modeling and optimization of UAV measurements for mobile communications using the L-SHADE algorithm," *IEEE Trans. Antennas Propag.*, vol. 67, no. 6, pp. 4022–4031, Jun. 2019, doi: 10.1109/TAP.2019.2905665.

[53] *MATLAB and Statistics Toolbox Release 2017b*, MathWorks, Natick, MA, USA, 2017.

[54] L. Babani, S. Jadhav, and B. Chaudhari, "Scaled conjugate gradient based adaptive ANN control for SVM-DTC induction motor drive," in *Proc. IFIP Int. Conf. Artif. Intell. Appl. Innov.* Cham, Switzerland: Springer, Sep. 2016, pp. 384–395.

[55] A. A. Bataineh and D. Kaur, "A comparative study of different curve fitting algorithms in artificial neural network using housing dataset," in *Proc. IEEE Nat. Aerosp. Electron. Conf. (NAECON)*, Jul. 2018, pp. 174–178.

Monica Kaushik (Graduate Student Member, IEEE) received the M.Tech. degree from Maharshi Dayanad University, Rohtak, India, in 2009. She is currently pursuing the Ph.D. degree with Amity University, Noida, India. She is also an Assistant Professor with the Department of Electronics and Communication Engineering, Amity School of Engineering and Technology, Amity University. Her research interests include wireless body area networks and *in vivo* body area networks.

Sindhu Hak Gupta received the Ph.D. degree from the Department of Electronics and Communication Engineering, Faculty of Engineering and Technology, Uttarakhand Technical University, Dehradun, India, in 2016. She is currently an Associate Professor with the Department of Electronics and Communication Engineering, Amity School of Engineering and Technology, Amity University, Noida, India. Her research interests include energy efficient wireless sensor networks, efficient body area networks, and cooperative communication.

Vipin Balyan received the B.E. (Hons.) degree in electronics and communication in 2003, the M.Tech. degree in electronics and networking from LaTrobe University, Melbourne, VIC, Australia, in 2006, and the Ph.D. degree in efficient single code assignment in OVSF-based WCDMA wireless networks in 2013. He is currently working with the Department of Electrical, Electronics and Computer Engineering, Cape Peninsula University of Technology, Bellville Campus, Cape Town, South Africa. He is an NRF, South Africa Rated Researcher. His research interests include CDMA, OFDM, VSF-OFCDM, and GFDM.